Supramolecular hydrogel-based protein and chemosensor array†

Masato Ikeda,[a] Rika Ochi[a] and Itaru Hamachi*[ab]

Received 7th April 2010, Accepted 9th July 2010
DOI: 10.1039/c004908e

The development of protein and sensor arrays is crucial for rapid and high-throughput assays of biological events, markers, environmental pollutants, and others. We describe supramolecular hydrogel as a unique material for use as a matrix for immobilizing proteins, peptides, substrates, chemosensors, and mesoporous silica particles, and thereby array them on solid supports. The semi-wet conditions provided by the gel, which consists of 3D supramolecular nanofiber network structure, are suitable for entrapping such substances whilst retaining their activity and function. Moreover, the hydrophobic interior of the nanofibers of the supramolecular hydrogel can reversibly entrap hydrophobic molecules, which allows the development of various read-out systems, such as fluorescence enhancement and fluorescence resonance energy transfer (FRET), by which one can monitor the signal changes associated with, for instance, molecular recognition and enzyme activity.

1. Introduction

Array technologies using immobilized artificial- or bio-molecules on solid supports undoubtedly exhibit several advantages over solution-based analyses. Such arrays, constructed using plain glass slides, are easily handled and readily applicable to rapid screening with minimal sample usage. Thus, various types of DNA/protein/peptide/saccharide arrays are now being developed for rapid and high-throughput analysis of a wide range of biological substances.[1–4] As evidenced by DNA microarrays, these arrays or chips are potentially versatile not only for fundamental research, but also for medical diagnosis or personal medicine in the future. In most array technologies, however, immobilization of bio-molecules on the surface of solid substrates undergoes a drying process and involves inevitable chemical processes for covalently attaching the materials to a substrate. Such unnatural circumstances confer unfavorable effects on immobilized bio-macromolecules, which results in reducing the sensing capability of these microarrays in some cases. We have recently developed novel hydrogels consisting of self-assembled small molecules (so-called 'supramolecular hydrogels') and proposed these are useful materials for immobilizing artificial- or bio-molecules under semi-wet conditions without drying or tedious chemical processes. These gels consist of a 3D network of nanofibers constructed from low-molecular-weight molecules (hydrogelators) *via* multiple non-covalent interactions.[5–7] In this review, we describe that supramolecular

[a]*Department of Synthetic Chemistry and Biological Chemistry, Graduate School of Engineering, Kyoto University, Katsura, Kyoto, 615-8510, Japan. E-mail: ihamachi@sbchem.kyoto-u.ac.jp*
[b]*Japan Science and Technology Agency (JST), CREST, 5 Sanbancho, Chiyoda-ku, Tokyo, 102-0075, Japan*
† Published as part of a LOC themed issue dedicated to Japanese Research: Guest Editor Professor Yoshinobu Baba

Masato Ikeda

Assistant professor Masato Ikeda was born in 1975 in Ehime, Japan. He received his PhD from Kyushu University in 2002. In 2003–2004, he carried out JSPS post-doctoral research at ISIS (University of Louis Pasteur) in France. In 2004–2006, he joined the Yashima Super-structured Helix Project (ERATO, JST) in Nagoya as a post-doctoral researcher. In 2006, he became an assistant professor at Kyushu University. In 2007, he joined Kyoto University as an assistant professor. His research interests focus on supramolecular materials chemistry based on self-assembled nanostructures and molecular machines.

Rika Ochi

Rika Ochi was born in 1983 in Ehime, Japan. She received her BS and MS degrees from Hokkaido University in 2007 and 2009, respectively. She is currently a PhD student at Kyoto University. Her research interests focus on bioorganic chemistry and supramolecular biomaterials.

hydrogel is a suitable and unique materials to be used as a matrix for immobilizing many kinds of bio- and artificial-materials on a solid support to afford functional protein/peptide or chemosensor arrays. Employment of the supramolecular hydrogel as a matrix offers several advantages. Firstly, the semi-wet conditions allows us to entrap and array bio-macromolecules such as proteins whilst maintaining their functions. Functional protein arrays, in which proteins keep their biological activities, are generally difficult to construct, compared with DNA arrays because of the easy denaturation and deactivation of many proteins through drying and chemical processes. Secondly, the signal/noise ratio for sensing may be greatly improved relative to 2D-surface systems since the micro-spaces formed by the nanofiber network can be accumulated in a 3D manner. Finally and uniquely, self-assembled nanofibers in the supramolecular hydrogel provide continuous hydrophobic spaces to capture hydrophobic molecules reversibly, in sharp contrast to conventional polymer hydrogels, and allows us to explore designable read-out systems using techniques such as environmentally-sensitive fluorescence enhancement and fluorescence resonance energy transfer (FRET).

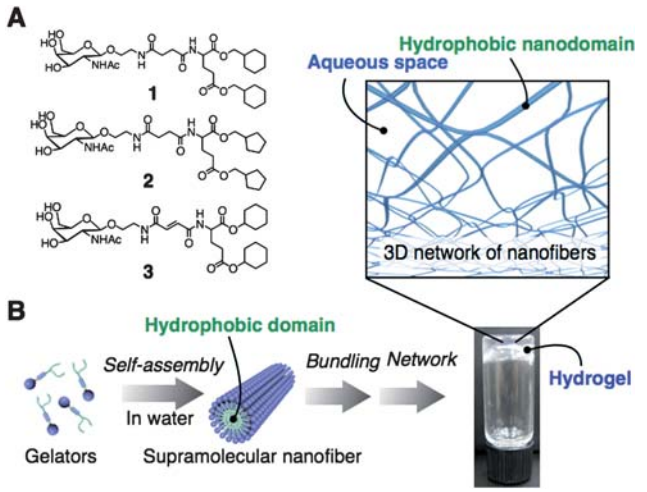

Fig. 1 **(A)** Chemical structures of hydrogelators (**1**, **2**, **3**). **(B)** Schematic illustration showing supramolecular hydrogel formation comprising self-assembled supramolecular nanofibers.

Itaru Hamachi

Professor Itaru Hamachi was born in 1960 in Fukuoka, Japan. He received his PhD from Kyoto University in 1988. He joined the faculty of Kyushu University as an assistant Professor in 1988, and was promoted to be an associate Professor at Kyushu University in 1992. In 2001, he became a full Professor at Kyushu University and then moved to Kyoto University in 2005. His research interests include biomolecular chemistry, nanobiochemistry and engineering, supramolecular chemistry and chemical biology.

We prepared a library of candidates of supramolecular hydrogelators and discovered some excellent low-molecular weight hydrogelators **1**,[8] **2**,[8] and **3**[9,10] as shown in Fig. 1, which can form stable and transparent hydrogels. Based on spectroscopic analysis and microscopic observation, we clearly demonstrated that these hydrogelators are self-assembled to form supramolecular nanofibers, which bundle to form a 3D network fixing a large amount of water inside. The formation of supramolecular hydrogels proceeds without additional chemicals. Simply, the aqueous sol obtained by gentle heating of an aqueous suspension containing the hydrogelator (white powders) gives rise to a hydrogel at room temperature, typically several minutes incubation are required (critical gel concentrations of **1**, **2**, and **3** are 0.1, 0.3, and 0.05 wt%, respectively. The gel–sol transition temperatures, at which the gel dissolves, are 48 °C (0.35 wt%) and 63 °C (0.10 wt%) for **2** and **3**, respectively. Hydrogelator **1** shows a unique phase transition behavior induced by temperature (phase transition temperature is 69 °C (0.27 wt%), which is similar to that of cross-linked poly-*N*-isopropyl-acrylamide[8]). The hydrogel formations are reversible and recyclable. It is also beneficial that these hydrogels can be stably prepared under various conditions, that is, under wide ranges of pH and salt concentration. This is critically important to entrap biomolecules such as enzymes whilst retaining their natural functions.[11] Furthermore, since the surface of the nanofibers is coated by hydrophilic sugar derivatives, it is reasonably expected that the nanofibers would have no deteriorated influences on the stability and/or functions of bio-macromolecules.

2. Semi-wet protein array using supramolecular hydrogel

2.1 Peptide/protein arrays

Protein arrays are now being actively developed to evaluate the activities of various proteins in a high-throughput manner.[2,12] The type and amount of natural proteins are direct indicators in many biological phenomena related to human health and diseases. In addition, proteins are anticipated as excellent scaffolds for analyzing a variety of biological substances through their highly sophisticated molecular recognition functions. However, compared to DNA arrays, preparation of functional protein arrays and chips is usually difficult due to the fragility of proteins under conventional drying processes. In particular, enzymes are generally more delicate than DNA and chemical compounds. Therefore, functional protein arrays are usually prepared by immobilizing proteins (enzymes) in buffers containing a high percent of glycerol onto a treated glass slide to maintain the wet environment.[13,14,15] However, there will be a certain influence of the glycerol on the activity of the proteins. By contrast, hydrogels are regarded as an intermediate between the dry and wet systems and they contain a large amount of fixed water (>99%). Therefore, we reasoned that usage of hydrogels as a matrix to immobilize proteins with retained functions may overcome this problem.

To evaluate the activity of entrapped enzymes in supramolecular hydrogel on the surface of a glass slide, we initially

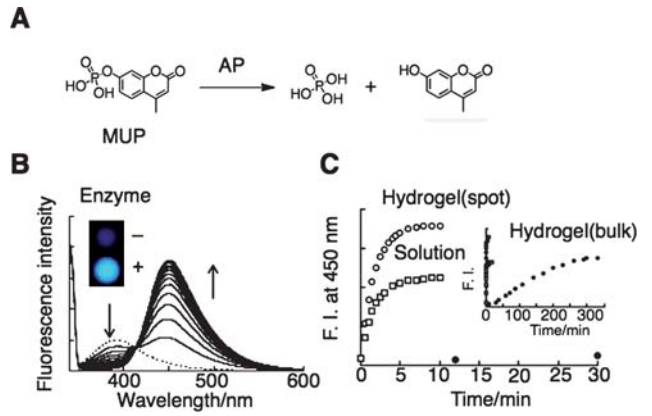

Fig. 2 **(A)** AP-catalyzed hydrolysis of fluorogenic substrate MUP.[16] **(B)** Fluorescence spectral changes for the AP-catalyzed hydrolysis of MUP in the hydrogel **1** and the corresponding change in the emission color of the hydrogel chip (inset, spot size is 4 mm in diameter). The broken line shows the spectrum of MUP in the absence of AP. **(C)** Time course for the change in fluorescence intensity at 450 nm for the AP-catalyzed hydrolysis of MUP. (○) 20 μL of the hydrogel **1** on a glass plate, (□) in aqueous solution, and (●) 100 μL of bulk hydrogel **1**. Conditions: [**1**] = 0.25 wt%, [AP] = 0.1 nM, [MUP] = 20 μM in 50 mM Tris-HCl buffer (pH 9.0) at RT (room temperature), λ_{ex} = 333 nm.

monitored the enzyme activity using a fluorogenic substrate.[16] As a typical example, alkaline phosphatase (AP), a hydrolytic enzyme, and a coumarin monophosphate (4-methylumbelliferyl phosphate, MUP), which is a standard substrate for AP, were used (Fig. 2A). When AP was added to gel **1** containing MUP, a rapid increase in the fluorescence intensity at 450 nm and decrease at 385 nm were observed, which can be ascribed to MUP being converted to strongly fluorescent hydroxycoumarin through the AP-catalyzed cleavage of a phosphoester bond (Fig. 2B). A similar fluorescence increase took place upon addition of MUP to the hydrogel immobilizing AP. It is worth noting that minimizing the size of the hydrogel spots to several tens of microlitres accelerated the apparent reaction rate in the gel to be almost comparable to that in aqueous media (Fig. 2C), and thereby a serious problem arising from slow diffusion of molecules inside the gel was solved. The same types of fluorescent responses were obtained for other pairs of enzymes and substrates (β-glucosidase and a coumarin-appended glucose (4-methylumbelliferyl-β-D-glucopyranoside: MUGlc), β-galactosidase and a coumarin-appended galactose (4-methylumbelliferyl-β-D-glucopyranoside: MUGal), and thrombin and a tripeptide-containing aminocoumarin at the *C*-terminal of Arg).[16] These results clearly demonstrated that the aqueous space fixed inside the supramolecular hydrogel has suitable properties for immobilizing naturally occurring enzymes whilst retaining their activity.

In addition to the aqueous space for enzyme encapsulation, hydrophobic domains of the supramolecular nanofibers seem potentially useful for capturing hydrophobic molecules. We indeed noticed that environmentally sensitive fluorophores, such as ANS (1-anilinonaphthalene-8-sulfonic acid) or DANSen (5-dimethylaminonaphthalene-1-(*N*-2-aminoethyl) sulfonamide) exhibited stronger fluorescence, upon mixing with supramolecular hydrogel, compared with that of the probe in aqueous solution (Fig. 3A).[8,17] By confocal laser scanning microscopy (CLSM), we confirmed that the entangled fiber network in the

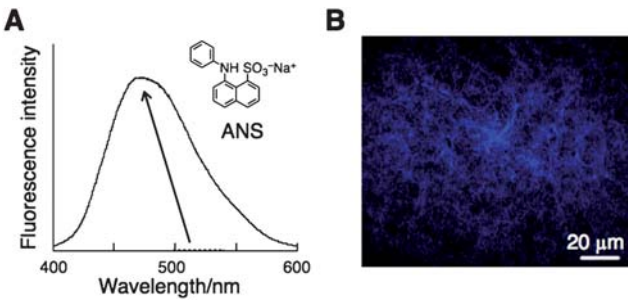

Fig. 3 **(A)** Fluorescence spectra of hydrogel **1** and aqueous solution containing ANS (solid line: hydrogel; dotted line: solution).[17] **(B)** CLSM image of hydrogel **1** containing ANS. Conditions: **A**: [ANS] = 10 μM in 25 mM phosphate buffer (pH 8.0), [**1**] = 0.25 wt%, λ_{ex} = 380 nm; **B**: [ANS] = 20 μM in H_2O, [**1**] = 0.13 wt%, λ_{ex} = 351 nm.

hydrogel was fluorescently stained with ANS, clearly indicating that the supramolecular fiber possessed continuous hydrophobic domains where ANS had accumulated (Fig. 3B). One may expect that the hydrophobic domains of the supramolecular hydrogels are valuable as a unique site for monitoring an enzyme reaction, if the enzyme-triggered change was induced by the hydrophobicity of the substances.

In a proof-of-principle experiment, a substrate for lysyl-endopeptidase (LEP) or trypsin (Tryp) was designed: a hydrophilic oligopeptide (**pep-1**) tethered to an environmentally sensitive fluorophore (DANSen) at the *C*-terminal of Lys (Fig. 4A).[17] When LEP cleaves the peptide bond between Lys and DANSen, the resultant DANSen possibly moves from the aqueous space to the hydrophobic domain because of DANSen's strong hydrophobicity, which may cause the fluorescence increase. Indeed, the emission intensity of **pep-1** immobilized in the supramolecular hydrogel **1** clearly increased along with a blue-shift by addition of LEP (Fig. 4B).[17] Interestingly, this color change can be detected by naked eye. In contrast, the addition of chymotrypsin (Chym) did not induce such a fluorescence change (Fig. 4C). The CLSM images strongly support the phenomenon that translocation of the fluorescent probe is triggered by the enzymatic hydrolysis. Fig. 4D shows a typical time-dependent change in the CLSM image of the supramolecular hydrogel containing **pep-1** during Tryp hydrolysis.[16] Before Tryp addition, the image was rather dark and the weak emission was smeared. During the initial stage of the reaction (within 10 s), many dispersed bright spots appeared that were not connected to each other. After 100 s, the spots became continuous and fibrous networks with strong emission were observed. These results directly revealed that the present supramolecular hydrogel restores the substantial fluidity and therefore provides a unique medium for sensing the enzyme activity.

The product redistribution triggered by enzymatic reaction can be extended to the rational design of a FRET-type read-out mode for enzyme activity in the gel chip.[16] As a suitable FRET pair, a coumarin-appended peptide **pep-2** (Chym, Tryp, or LEP enzyme substrate), and a hydrophobic styryl dye **4** as an acceptor for coumarin emission, were embedded together in the supramolecular hydrogel (Fig. 5A). Fig. 5B shows the fluorescence change during the hydrolysis by Chym. Upon the addition of Chym, the peak at 514 nm (coumarin) decreased and the peak at 594 nm (styryl dye) increased (F_{594}/F_{514} changed from 1.06 to

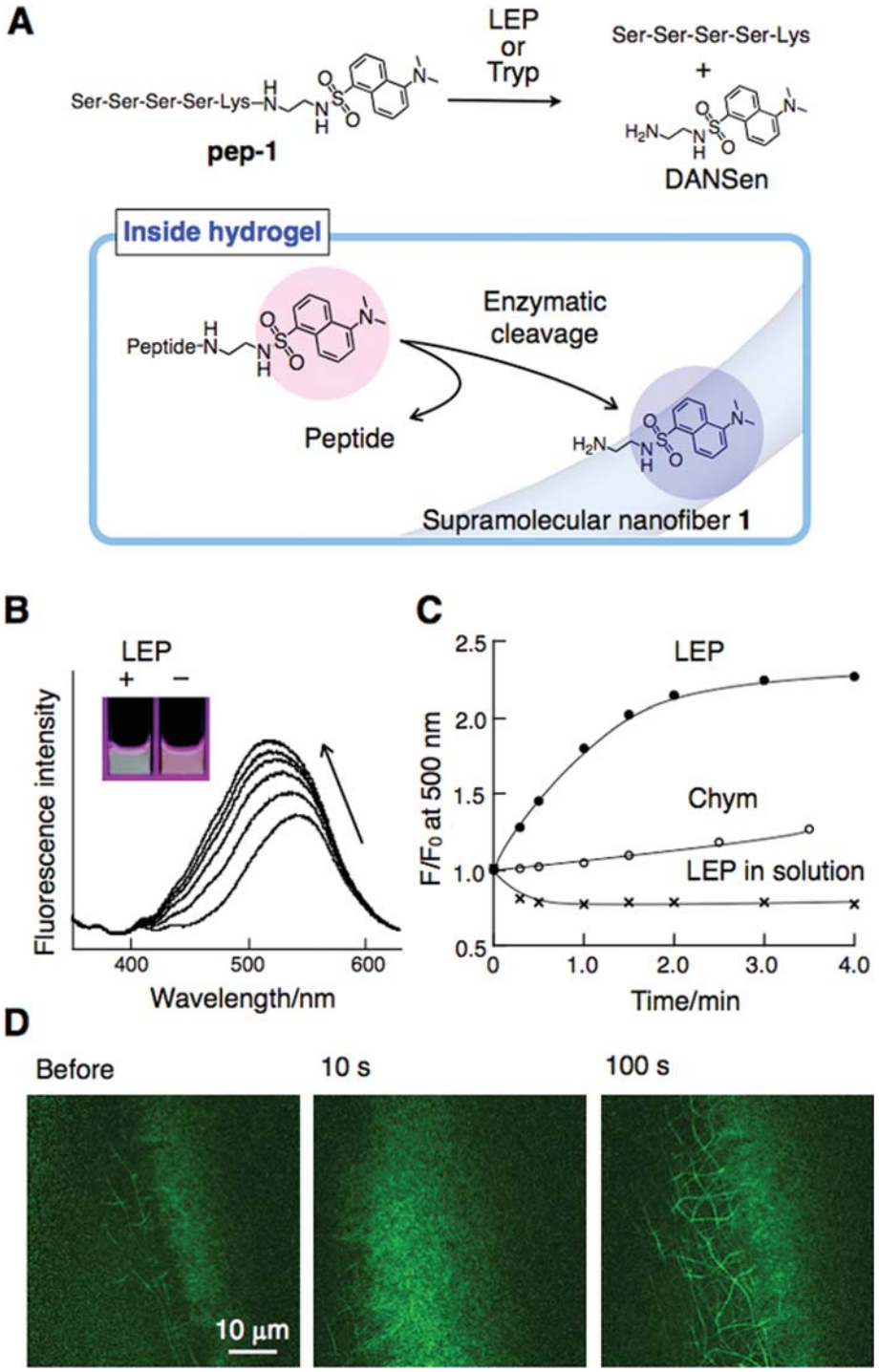

Fig. 4 **(A)** Chemical structure of a peptide substrate (**pep-1**) and the mechanism of the enzymatic hydrolysis of **pep-1** in the hydrogel **1**.[16,17] The cleaved dansyl fragment (DANSen) is distributed into the hydrophobic space of the nanofibers, which results in enhancement of the fluorescence of DANSen along with a blue shift of the fluorescence wavelength. **(B)** Fluorescence spectral change of **pep-1** embedded in the hydrogel **1** by enzymatic (LEP) hydrolysis and the corresponding emission color change (inset). **(C)** Time course for the change in fluorescence intensity at 500 nm. **(D)** CLSM images of the trypsin-catalyzed hydrolysis of **pep-1** in the hydrogel **1**. Conditions: [**1**] = 0.25 wt%, **B**, **C**: [**pep-1**] = 20 μM, [LEP] = 500 nM in 50 mM Tris-HCl buffer (pH 8.5) at 37 °C, λ_{ex} = 330 nm; **D**: [Tryp] = 1 μM, [**pep-1**] = 100 μM in 50 mM Tris-HCl buffer (pH 8.0) containing 100 mM $CaCl_2$ at RT, λ_{ex} = 351 nm.

1.70). This seesaw type of spectral change indicated the facilitated FRET between the coumarin and the styryl dye, which is explained as follows: after hydrolysis, the cleaved coumarin fragment transfers to the hydrophobic domain because of its increased hydrophobicity, and as a result, the average distance between the two fluorophores is reduced to enhance the FRET efficiency. By contrast, in the absence of the FRET acceptor (**4**), a significant change in the fluorescence spectra was not observed (Fig. 5C). Apparently, using a FRET-type read-out mode, clearer signal discrimination can be achieved than simple environmental probes.

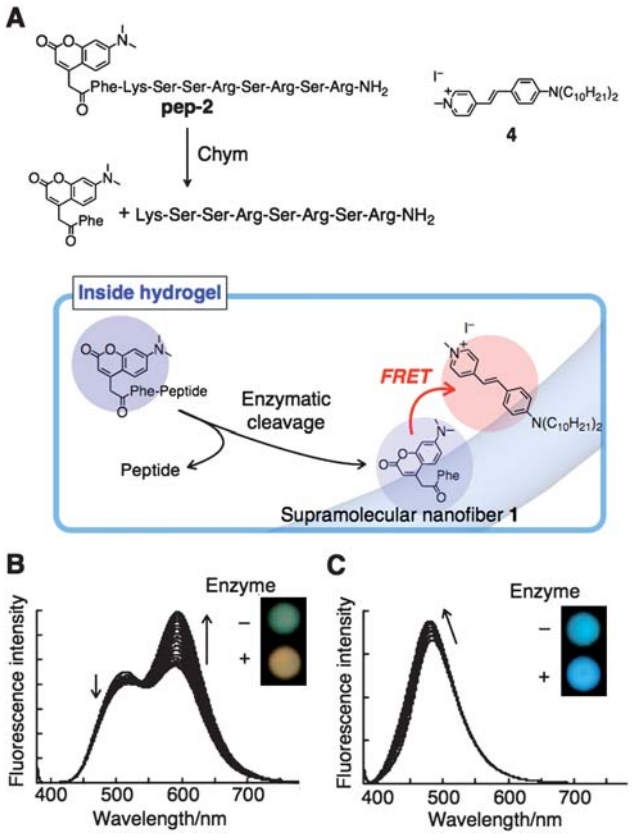

Fig. 5 **(A)** Chemical structure of a peptide substrate (**pep-2**) and FRET acceptor (**4**) and mechanism for the FRET process in the enzymatic reaction in the hydrogel **1**. **(B)** Fluorescence spectral change for the chymotrypsin-catalyzed hydrolysis of **pep-2** in the hydrogel containing **4** and the corresponding emission color change of the hydrogel chip (inset, spot size is 4 mm in diameter). **(C)** Fluorescence spectral change for the chymotrypsin-catalyzed hydrolysis of **pep-2** in the hydrogel in the absence of **4** and the corresponding emission color change of the hydrogel chip (inset, spot size is 4 mm in diameter). Conditions: [**1**] = 0.25 wt%, [Chym] = 1 μM in 50 mM Tris-HCl buffer (pH 8.0) containing 100 mM $CaCl_2$ at RT, λ_{ex} = 351 nm, **B**: [**pep-2**] = 100 μM, [**4**] = 200 μM; for **C**: [**pep-2**] = 100 μM. For more detailed conditions, see ref. 16.

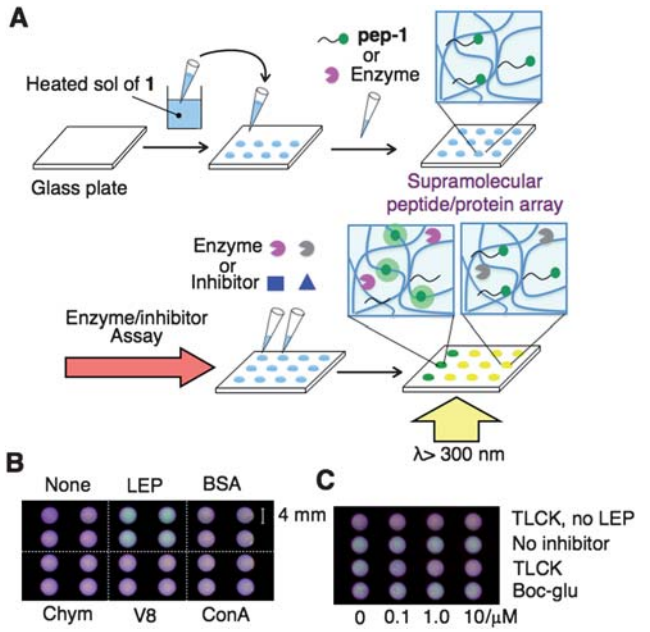

Fig. 6 **(A)** Preparation scheme of supramolecular peptide/protein array. **(B)** Fluorescent enzyme activity assay using a supramolecular hydrogel-based peptide chip. **(C)** Assay of LEP inhibitors using supramolecular hydrogel-based protein chip. Conditions: [**1**] = 0.25 wt%, **B**: ([**pep-1**] = 20 μM, [enzyme or protein] = 0.5 μM in 50 mM Tris-HCl buffer (pH 8.0) at RT; **C**: [**pep-1**] = 40 μM, [LEP] = 1.0 μM, [inhibitor] = 0, 0.1, 1.0, 10 μM in 50 mM Tris-HCl buffer (pH 8.5) at RT. Boc-glu, where Boc is *t*-butoxycarbonyl, is another inhibitor but not potent for LEP. For more detailed conditions, see ref. 17.

These hydrogel spots were aligned on a glass plate (Fig. 6A), so that one can construct a peptide and protein array chip for high-throughput screening of enzyme function. As shown in Fig. 6B, the gel chip containing **pep-1** showed bright green emission, only at spots injected with LEP. The addition of other proteins, all of which were not capable of cleaving **pep-1**, did not cause any fluorescence changes. Alternatively, a protein array can be prepared by injection of LEP into the supramolecular hydrogel spots before addition of **pep-1**. Using this protein chip, we can successfully assay an inhibitor for LEP (TLCK, N^{α}-tosyl-lysine chloromethylketone). As shown in Fig. 6C, in the absence of the inhibitor, the gel spot showed bright green emission, whereas the emission from spots containing the inhibitor became smeared, depending on the inhibitor concentration.

2.2 Lectin array

Such semi-wet protein arrays were not restricted to enzymes, but extended to ligand-binding proteins. In this section, we focus on a novel lectin (a family of sugar-binding proteins) array for analyzing glycoconjugates.[18] As sugars and their derivatives such as oligosaccharides, glycolipids, and glycoproteins play important roles in various biological phenomena,[19,20] the rapid and high-throughput analysis of diverse glycoconjugates is highly desirable. For this purpose, we attempted to construct a lectin-based fluorescence read-out system immobilized in the hydrogel matrix, which relied on a bimolecular fluorescence quenching and recovery (BFQR) technique,[21] comprising a fluorescein-labeled lectin (F-lectin) and corresponding sugar-appended dabcyl (4,4-dimethylamino-azobenzene-4′-carboxylic acid) as quencher (Q-sugar) (Fig. 7A,B). These BFQR constructs were non-covalently immobilized in the hydrogel **1**, where the embedded constructs were expected to act as fluorescence turn-on scaffolds for sensing specific sugars.

When we used fluorescein-labeled concanavaline A (F-Con A, a mannose and glucose binding lectin) as a F-lectin, mannobiose-appended dabcyl (Q-mannobiose, Q-sugar **5**) was selected as a paired Q-sugar. The fluorescence intensity of F-Con A immobilized in the hydrogel **1** substantially decreased by the addition of Q-mannobiose (**5**) and recovered by the addition of mannotriose (Man-tri), the strongest ligand of Con A (Fig. 7C). On the other hand, the quenched fluorescence did not recover by sugars such as galactose or lactose which does not bind Con A. Similarly, other pairs can be used in the lectin array, that is, F-lectins showing distinct sugar selectivity (WGA (β-GlcNAc, α2,3-Neu-NAc), GSL-II (α,β-GlcNAc), AAL (Fuc), UEA-1 (α1,2-Fuc), GSL-1 (α-Gal, GalNAc), where sugar selectivity is shown in

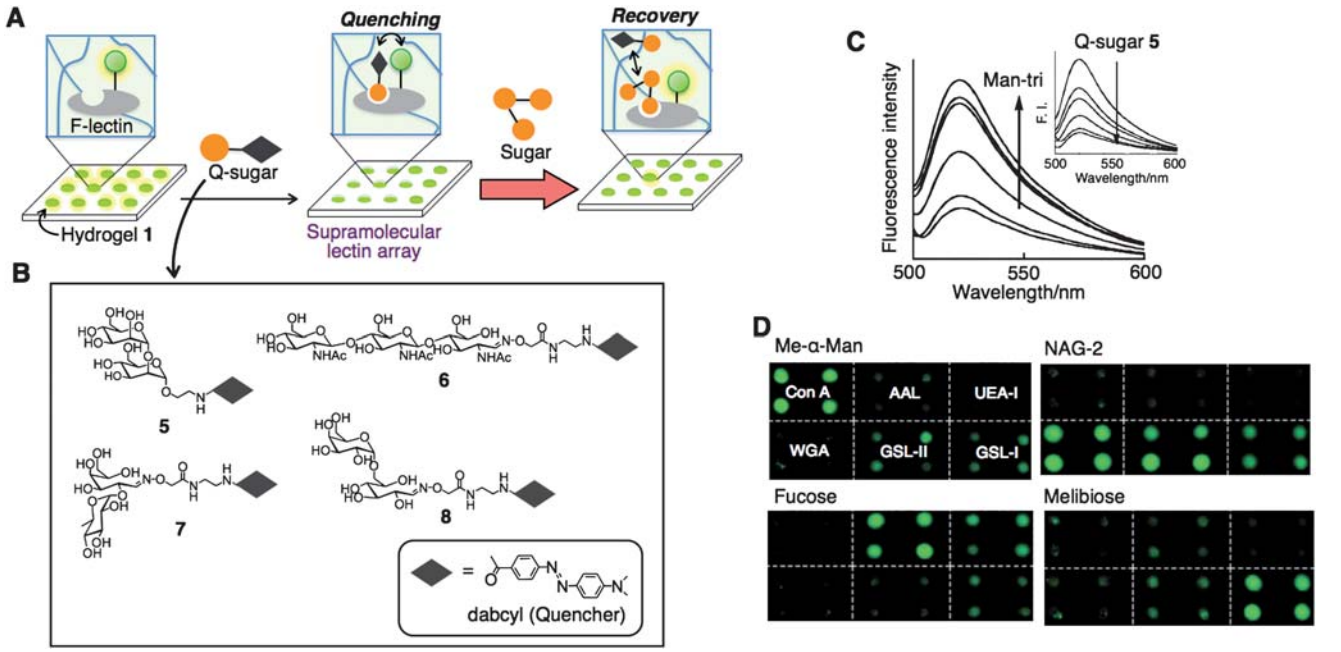

Fig. 7 **(A)** Schematic illustration showing construction of BFQR fluorescent detection system on hydrogel chip. **(B)** Chemical structures of quenchers (Q-sugar). **(C)** Fluorescence recovery of F-Con A immobilized in the hydrogel **1** by the addition of Man-tri and fluorescence quenching process (inset) of F-Con A upon addition of Q-sugar **5**. **(D)** Fluorescent sugar sensing using a supramolecular hydrogel-based lectin chip (spot size is 4 mm in diameter) (Me-α-Man (methyl-α-mannose), NAG-2 (*N*,*N*′-diacetyl chitobiose), fucose, and melibiose. Conditions: [**1**] = 0.25 wt% in 50 mM HEPES buffer (pH 7.5) containing 1 mM $MnCl_2$, 1 mM $CaCl_2$, and 100 mM NaCl, **C**: ([F-Con A] = 1 μM, [Man-tri] = 0–1.0 mM, [**5**] = 0–10 μM, λ_{ex} = 475 nm; **D**: [sugar] = 10 mM, [F-Con A] = 0.1 μM, [**5**] = 1 μM; [F-WGA] = 0.1 μM, [**6**] = 2.0 μM; [F-GSL-II] = 0.1 μM, [**6**] = 30 μM; [F-AAL] = 0.1 μM, [**7**] = 1 μM; [F-UEA-I] = 0.1 μM, [**7**] = 10 μM; [F-GSL-I] = 0.1 μM, [**8**] = 30 μM, for more detailed conditions, see ref. 18.

parentheses) and the corresponding Q-sugars (**6**, **7**, **8**). As shown in Fig. 7D, the sugar paired to each lectin can induce the enhancement of fluorescence, which allows us to distinguish it among sugars in each solution spotted to the hydrogel chip. Not only simple sugars, but also the branched sugar and glycoproteins can be roughly characterized by this lectin array. Furthermore, the more complicated analytes, cell lysates of different cell lines, were successfully profiled on the basis of the fluorescence response pattern using the lectin array.

3. Semi-wet artificial sensor arrays using supramolecular hydrogel

3.1 Fluorescent sensor arrays

Not only peptides and proteins, but also artificial chemosensors can be embedded in the supramolecular hydrogel spots to afford a chemosensor array. As one representative, a fluorescent chemosensor **9** (Fig. 8A(a)), which was originally developed to detect phosphate and its derivatives by fluorescence enhancement,[22,23] was immobilized in supramolecular hydrogel **2** (Fig. 8A(b)).[24] We demonstrated that the chemosensor **9** inside the gel matrix **2** retained almost the same sensing function as in aqueous solution; that is, the fluorescence enhancement occurred for phosphates such as phenyl phosphate (PhP: $K = 6.2 \times 10^4$ M^{-1}, $F/F_0 - 1 = 2.2$) and phospho-tyrosine (p-Tyr: $K = 2.0 \times 10^5$ M^{-1}, $F/F_0 - 1 = 4.5$) (Fig. 8B(a),(b)), whereas other anions such as sulfate, nitrate, and acetate did not cause any considerable fluorescence change (Fig. 8B(c)). In a similar manner, we demonstrated that other chemosensors such as Zn^{2+} probe **10**,[25] Ca^{2+} probe (CG-2),[26] and pH probe (SNARF-1)[27] can be embedded in a hydrogel spot with neither loss of their function, nor any chemical modification. For rapid and efficient sensing, the four fluorescent chemosensors immobilized in a supramolecular hydrogel were integrated onto one glass plate to produce a chemosensor array, that is, a molecular recognition chip. Four distinct analytes, phosphorylated peptide (p-pep), Zn^{2+}, Ca^{2+}, and pH were simultaneously analyzed from the mixed solution without being disturbed by the other analytes (Fig. 8B(d)). These results indicate that the present molecular recognition chip is potentially applicable to mixed sample analysis without tedious isolation processes.

Many artificial chemosensors that can sense a variety of analytes, have been developed so far.[28,29] To construct a sensor array employing such artificial chemosensors, the chemosensors were conventionally embedded in solid supports such as a polymer resin[30,31] or glass plates through covalent linkage. However, the sensors frequently suffered as their function was often suppressed by such immobilization.[32,33] This problem has prevented a lot of potentially useful chemosensors from practical applications. The present supramolecular entrapment method may facilitate more flexible usage of many existing chemosensors for array technology.

3.2 Molecular receptor array for discriminating phosphate and its derivatives

An elaborate chemosensory system can be designed using a simple phosphate receptor, which alone is not a chemosensor, if cooperative actions can be devised between the receptor and the

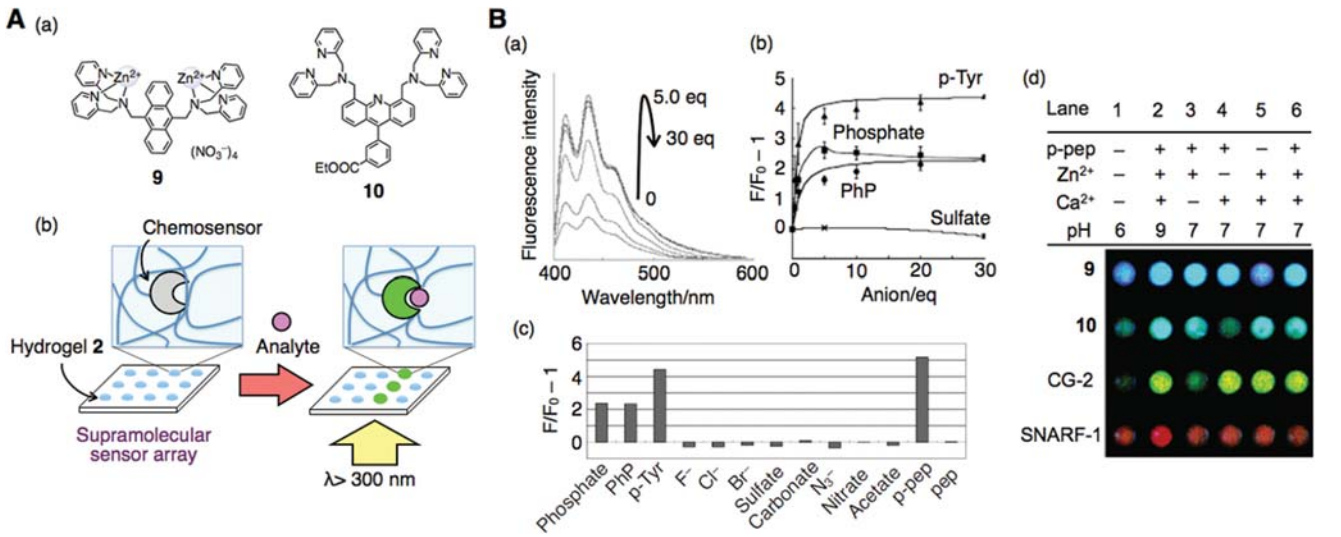

Fig. 8 **(A)** (a) Chemical structures of chemosensors (**9**, **10**) and (b) schematic illustration of sensing assay with supramolecular chemosensor array. **(B)** (a) Fluorescence spectral change of **9** embedded in hydrogel **2** upon addition of phosphate. (b) Fluorescence titration plots of **9** ($\lambda_{em} = 435$ nm) embedded in hydrogel **2** with various anions: PhP (●), p-Tyr (▲), phosphate (■), and sulfate (×). (c) The emission intensity change of a hydrogel array containing **9** upon the addition of various anions. (d) Fluorescent mixed solution assay using a supramolecular hydrogel-based molecular recognition chip (spot size is 4 mm in diameter). Conditions: [**2**] = 0.5 wt% in 50 mM HEPES (pH 7.2), **B**(a,b): [**9**] = 20 μM, [phosphate] = 0–600 μM, $\lambda_{ex} = 380$ nm; **B**(c): [**9**] = 40 μM, [anion] = 200 μM, $\lambda_{ex} = 380$ nm; **B**(d): [**9**] = 20 μM, [**10**] = 80 μM, [CG-2] = 50 μM (including [EDTA] = 1 mM), or [SNARF-1] = 10 μM from the top to bottom, six mixed solutions including [p-pep] = 0 (–) or 30 μM (+), [$Zn(NO_3)_2$] = 0 (–) or 120 μM (+), [$Ca(NO_3)_2$] = 0 (–) or 1 mM (+), pH 7.0 or 9.0, for more detailed conditions, see ref. 24. The sequence of p-pep is DEEI*p*YGEFF.

hydrophobic microdomain of a hydrogel matrix.[34] As a fluorescent receptor, a phosphate receptor **11** bearing two Zn/Dpa (dipicolyl-amine) moieties and an environmentally sensitive fluorophore (dansyl) was employed (Fig. 9A), the fluorescence of which never changed upon phosphate binding in homogeneous solution. Surprisingly, in contrast, two distinct fluorescence

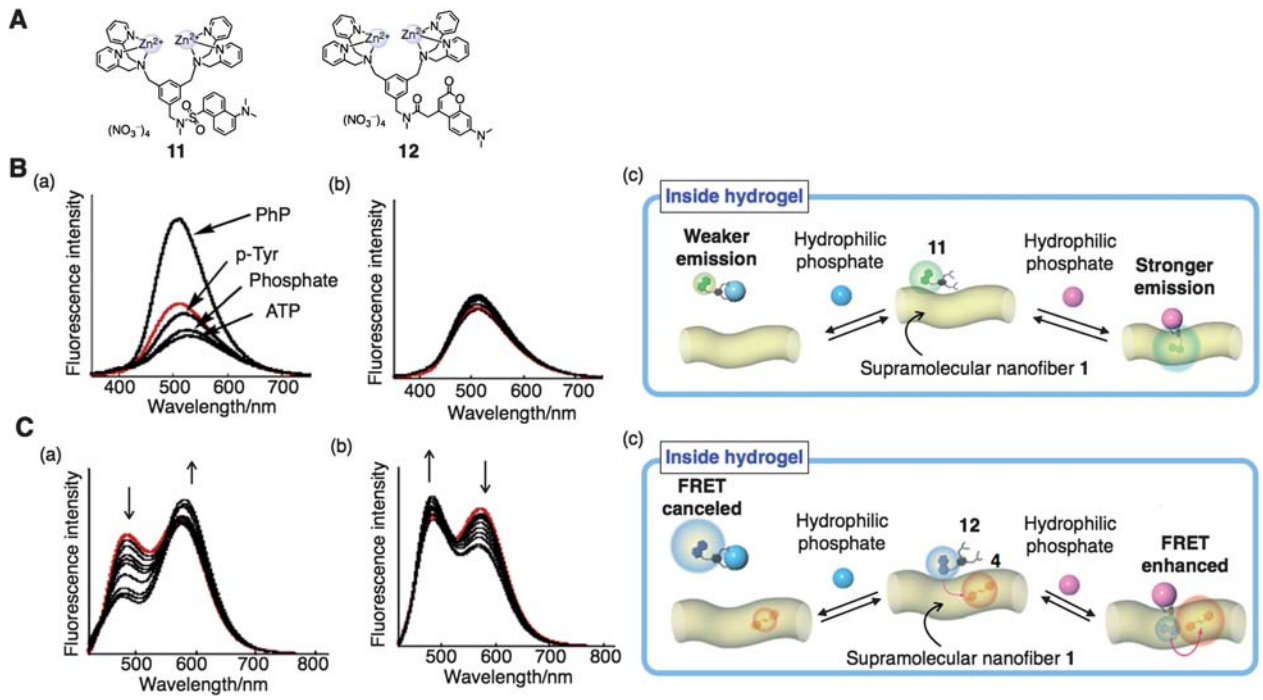

Fig. 9 **(A)** Chemical structures of receptors **11** and **12**. **(B)** (a) Fluorescence spectral change of **11** embedded in **1** upon addition of PhP, ATP, phosphate, and p-Tyr, (b) Fluorescence spectra in the presence of other non-phosphate anions (red lines: no guest), and (c) schematic illustration of the chemosensor redistribution upon the binding to hydrophobic or hydrophilic phosphate derivative between the hydrophobic supramolecular nanofiber and the hydrophilic cavity. **(C)** Fluorescence spectral change of the hydrogel **1** containing **12** and **4** in a titration of (a) PhP and (b) ATP (red lines: no guest). (c) Schematic illustration of the guest-dependent FRET system using **12** and **4** in the hydrogel matrix. Conditions: [**1**] = 0.5 wt% in 50 mM HEPES (pH 7.2), **B**(a,b): [**11**] = 60 μM, [anion] = 600 μM, $\lambda_{ex} = 322$ nm; **C**(a,b): [**12**] = 50 μM, [**4**] = 50 μM, [PhP], [ATP] = 0–500 μM, $\lambda_{ex} = 393$ nm.

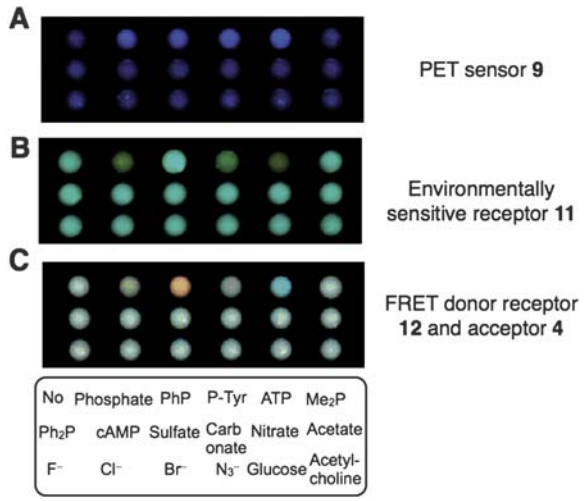

Fig. 10 Fluorescent sensing pattern assay using a supramolecular hydrogel-based molecular recognition chips (spot size is 4 mm in diameter). Conditions: [**1**] = 0.5 wt% in 50 mM HEPES (pH 7.2), **A**: [**9**] = 40 μM, [anion] = 200 μM; **B**: [**11**] = 60 μM, [anion] = 500 μM; **C**: [**12**] = 50 μM, [**4**] = 50 μM, [anion] = 600 μM, the spotted position of anions is shown at the bottom, for more detailed conditions, see ref. 34.

changes were observed when phosphate anion derivatives were added to **11** immobilized in the supramolecular hydrogel chip **1**. That is, the emission intensity of **11** (λ_{max} = 512 nm) increased with a blue-shift in the emission maximum for PhP (F/F_0 = 2.1, λ_{max} = 503 nm), whereas the intensity decreased with a red-shifted emission for adenosine triphosphate (ATP) (F/F_0 = 0.56, λ_{max} = 528 nm), phosphate (F/F_0 = 0.64, λ_{max} = 527 nm), and p-Tyr (F/F_0 = 0.87, λ_{max} = 523 nm) (Fig. 9B(a)). It is clear that the fluorescence response was closely associated with the hydrophilicity of the guest molecules; the hydrophobic phosphate (PhP) caused the blue-shift with the increased emission intensity, while the strongly hydrophilic phosphates (ATP, phosphate, and p-Tyr) induced a red-shift with a reduced emission intensity. A detailed investigation clarified the sensing mechanism as follows: the receptor **11** is loosely bound to the supramolecular nanofiber surface before the host–guest interaction. Upon binding to hydrophobic phosphate, it is more densely accumulated in the hydrophobic domain of the nanofiber, whereas it is more dispersed in the aqueous space of the hydrogel matrix by the binding of hydrophilic guest molecules (Fig. 9B(c)). Clearly, the nanofibers functioned as an effective signal transduction domain to monitor such a recognition process, so that the phosphate anion species may be discriminated from each other by using both the intensity change and the wavelength shift in the emission.

The guest-dependent redistribution of the artificial receptor can be rationally coupled with the FRET read-out system, so that more explicit sensing was carried out by the molecular recognition array, like the FRET type of peptide/protein array.[34] As a suitable FRET acceptor of the coumarin-appended receptor **12** (Fig. 9A), the styryl dye **4** (Fig. 5A) was embedded in the supramolecular hydrogel. With the addition of PhP, the peak at 485 nm (coumarin) decreased and the peak at 569 nm (styryl dye) concurrently increased (F_{569}/F_{485} changed from 1.1 to 2.5) (Fig. 9C(a)). On the other hand, with the addition of ATP, the peak at 485 nm increased and the peak at 569 nm decreased (F_{569}/F_{485} changed from 1.1 to 0.72) (Fig. 9C(b)). These seesaw types of spectral changes are typical of FRET.

For rapid and high-throughput sensing of phosphate derivatives, the three different molecular recognition chips employing chemosensor **9** and receptors **11** and **12** were constructed. In the case of the PET-type chemosensor **9** (Fig. 10A), it is apparent that the intensified blue fluorescence at the spots including phosphate, PhP, ATP, and p-Tyr can be distinguished.[24] In addition to the intensity change, the color change was induced for the environmentally sensitive dansyl-appended receptor **11** (Fig. 10B). The four spots including phosphate, PhP, ATP, and p-Tyr can be distinguished by the emission change, but the changing pattern is different from that of chemosensor **9**. For the FRET type of chip employing receptor **12**, the color of the hydrogel more clearly changed to orange at the spot of the PhP addition, or to bluish at the spot of the ATP addition (Fig. 10C).

3.3 Mesoporous material–enzyme hybrid array for polyanions

As well as phosphate anions, poly-sulfates are known to play a variety of biological roles *in vivo*.[35] For example, contamination

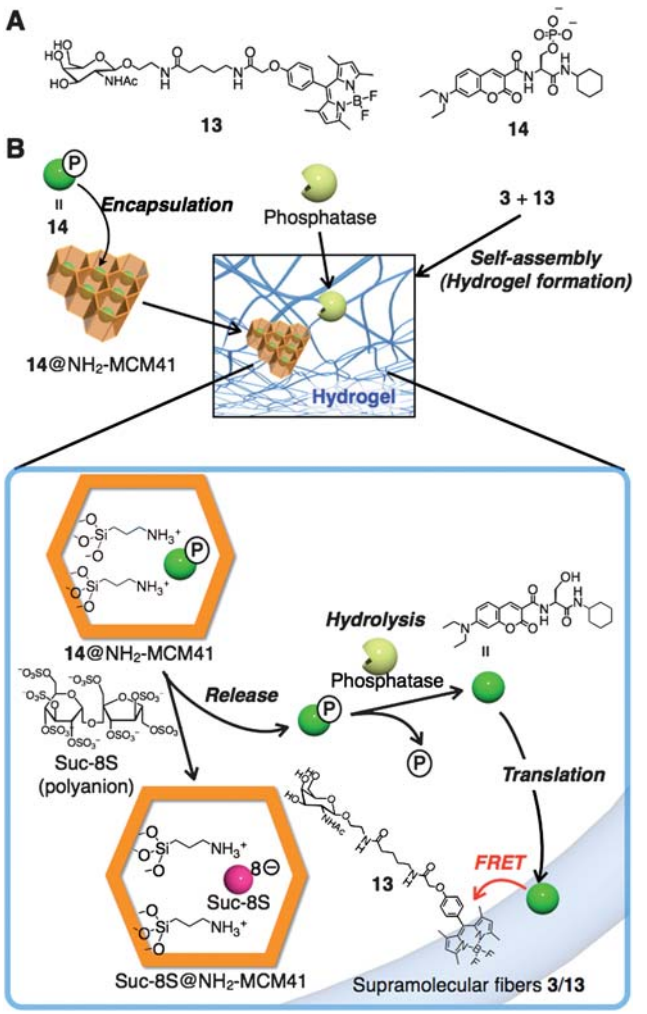

Fig. 11 **(A)** Chemical structures of BODIPY **13** and P-coum **14**. **(B)** Construction and mechanism operating in fluorescent dye encapsulated MCM-enzyme-supramolecular hydrogel hybrid sensory system.

by over-sulfated chondroitin sulfate in certain lots of heparin was recently reported to cause serious side effects presumably due to anaphylactoid response.[36] Thus, simple and selective detection of such poly-sulfates is now much in demand. A fluorescence sensing system for poly-sulfates was successfully constructed by a hybrid material consisting of supramolecular hydrogel, enzyme, and mesoporous silica particles (MCM41) encapsulating a fluorescent probe in the pores.[37] In this hybrid material, coupling of the polyanion-selective release of the fluorescent probe from MCM41[38] with the probe translocation to the supramolecular nanofiber facilitated by enzyme reaction yielded a unique FRET-type sensing material for polyanions.

Fig. 11 illustrates a strategy for the construction of the MCM–enzyme–supramolecular hydrogel hybrid sensor. We used aminopropyl-modified MCM41 (NH_2-MCM41)[39] that can encapsulate a phosphorylated serin appended coumarin (P-coum **14**) and release it by the anion exchange reaction triggered by poly-sulfates or poly-phosphates, but not by other substrates (poly-carboxylate, mono-anions, neutral, and cationic substrates). After the polyanion-triggered fluorophore release from NH_2-MCM41, the enzymatic cleavage of the phosphoester bond of P-coum **14** occurs in aqueous space, so as to alter the water-soluble P-coum **14** to the rather hydrophobic coumarin (Fig. 11B). The produced coumarin fragment was accumulated to the nanofibers, thereby the FRET mode of sensing was carried out.

CLSM images of the hybrid materials comprising NH_2-MCM entrapping P-coum **14** and hydrogel **3** revealed that aggregated NH_2-MCM41 (green fluorescence) and the supramolecular fibers (red fluorescence) can provide microdomains orthogonal to each other in the gel matrix (Fig. 12A). As shown in Fig. 12B, localization of the fluorescent probe was shifted in the hybrid gel before and after treatment with a poly-sulfate, sucrose octasulfate (Suc-8S), coupled with acid phosphatase (ACP). While the addition of only Suc-8S simply decreased the fluorescence intensity from the spots, the green fluorescent fibers were clearly visualized by the subsequent addition of ACP. We also confirmed that the translation of P-coum **14** never occurred without Suc-8S addition, even in the presence of ACP, suggesting that P-coum **14** when entrapped in the interior of NH_2-MCM41 is protected from enzymatic hydrolysis.

Such translocation of the fluorescent probe can be macroscopically detected using a FRET-type emission change, for which a FRET acceptor (BODIPY **13**) was additionally embedded in the hydrophobic domain of the hydrogel fibers. As shown in Fig. 12C(a), the emission at 483 nm from coumarin decreased, and the emission intensity at 513 nm from BODIPY concurrently increased. The change was saturated with increase in Suc-8S content (Fig. 12C(b)), clearly demonstrating the validity of the hybrid hydrogel as a fluorescent anion-sensing material. Interestingly, we noticed that 1,4,5-inositol-triphosphate (IP_3) and ATP were scarcely detected using this hybrid hydrogel despite the high anion-exchange activity. This might be ascribed to ACP immobilized in the hybrid gel rapidly hydrolyzes the phosphoester bonds of IP_3 and ATP, resulting in the reduction of their concentrations before anion exchange, which is a masking effect of ACP for such poly-phosphates. As a result, the present NH_2-MCM41-ACP hydrogel hybrid chip exhibited the improved selectivity for poly-sulfates relative to poly-phosphates.

In a hybrid materials array, bright emission was observed at spots containing inositol hexaphosphate (IP_6), heparin, Suc-8S, and chondroitin sulfate, but less bright emission came from

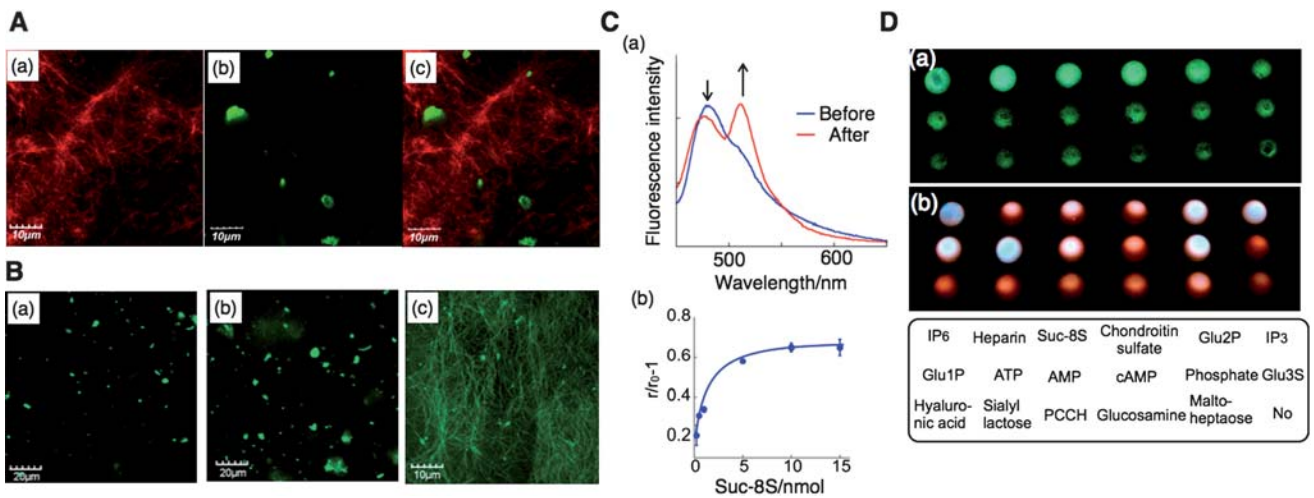

Fig. 12 **(A)** CLSM images of hydrogel **3** containing **13** and **14**@NH_2-MCM. The image (a) shows the localization of **13**, the image (b) shows the localization of **14**, and the merge image of (a) and (b) is shown in panel (c). **(B)** CLSM images tracing coumarin fluorescence in hydrogel **3** containing **14**@NH_2-MCM (a) before, (b) after 60 min of Suc-8S addition, and (c) after 90 min of subsequent ACP addition. **(C)** (a) Fluorescence spectral changes of hydrogel **3** containing **13** and **14**@NH_2-MCM before and after the addition of Suc-8S and ACP and (b) fluorescence titration plots for Suc-8S ($r/r_0 - 1 = (F_{513}/F_{483})/(F_{513}/F_{483})_0 - 1$). **(D)** Fluorescent polyanion sensing assay with a supramolecular hydrogel-based (a) MCM-enzyme hybrid sensor chip (spot size is 4 mm in diameter) containing **13** and **14**@NH_2-MCM, and ACP and (b) molecular recognition chip containing **12** and **4**. Conditions: [**3**] = 0.090 wt% in 200 mM acetate buffer (pH 5.0), λ_{ex} = 429 nm, **A**,**B**: [**13**] = 2.0 μM, [**14**@NH_2-MCM] = 9.0 mg mL^{-1}; **B**: [Suc-8S] = 1.15 mM; **C**: [**13**] = 3.0 μM, [**14**@NH_2-MCM] = 5.0 mg mL^{-1}, (a) [Suc-8S] = 1.4 mM; (b) [Suc-8S] = 0–1.4 mM (0–15 nmol); **D**(a): [**13**] = 3.0 μM, [**14**@NH_2-MCM] = 5.0 mg mL^{-1}, [anion] = 1.5 mM; **D**(b): [**3**] = 0.10 wt% in 50 mM HEPES (pH 7.2) containing 100 mM NaCl, [**12**] = 50 μM, [**4**] = 30 μM, [anion] = 0.5 mM, the spotted position of anions is shown at the bottom, for more detailed conditions, see ref. 37.

Table 1 Summary of supramolecular hydrogel-based array

Advantages	• Immobilization of artificial- or bio-molecules in semi-wet conditions whilst retaining their functions. • No concern about orientation of immobilized artificial- or bio-molecules • Easily prepared without tedious chemical processes • High signal/noise ratio due to 3D accumulation • Designable fluorescence read-out system
Disadvantages	• Not applicable to medium exchange process • Size-down issue due to high viscosity of hydrogel

others (Fig. 12D(a)). This is a contrast to a molecular recognition chip containing phosphate receptor **12** and the FRET acceptor **4** (Fig. 12 D(b)), where the spot colors of poly-phosphates changed, but the color change was not induced by poly-sulfates. Thereby, simple comparison between the response patterns of these two chips allows us to discriminate poly-sulfates such as heparin and Suc-8S from poly-phosphates such as IP_6 and ATP. These results implied that the rational hybridization of the anion-exchange ability of NH_2-MCM41 and the semi-wet supramolecular hydrogel matrix successfully produced a unique sensing array selective to poly-anions.

4. Conclusions and further remarks

We briefly discussed, using several examples, that supramolecular hydrogels are a novel semi-wet soft matrix for a variety of bio- and artificial-sensors arrays. Significantly, both the segregated aqueous nanospace and supramolecular nanofibers allow us to integrate programmable signal read-out systems (fluorescence enhancement, FRET) for enzymatic reactions, ligand-binding, and replacement events corresponding to the target substances inside the hydrogel. Although fairly successful so far, several issues should be improved for supramolecular hydrogel array systems (Table 1). For instance, the selection of environmentally sensitive dyes and FRET pairs is crucial to obtain sufficient signals, and thus screening of dyes is required in some cases. Also, to construct microarrays, utilization of a microarrayer or printing robot is inevitable. Although we demonstrated that supramolecular hydrogels **3** can be down-sized to a droplet of 60 pL in oil,[10] the combination of stimuli-responsive supramolecular hydrogels and spotting devices to induce stimuli at a desired time and place would be essential to construct microgels and microarrays reproducibly. We thus believe the fruitful combination of microfluidic and MEMS technologies with supramolecular hydrogel-based materials would become more important to find various future applications in the field of materials and bioanalytical science and explore new and practical devices.

References

1 M. Schena, D. Shalon, R. W. Davis and P. O. Brown, *Science*, 1995, **270**, 467–470.
2 T.-Y. Tomizaki, K. Usui and H. Mihara, *ChemBioChem*, 2005, **6**, 782–799.
3 D. Wang, S. Liu, B. J. Trummer, C. Deng and A. Wang, *Nat. Biotechnol.*, 2002, **20**, 275–281.
4 A. W. Martinez, S. T. Phillips and G. M. Whitesides, *Anal. Chem.*, 2010, **82**, 3–10.
5 L. A. Estroff and A. D. Hamilton, *Chem. Rev.*, 2004, **104**, 1201–1217.
6 M. de Loos, B. L. Feringa and J. H. van Esch, *Eur. J. Org. Chem.*, 2005, 3615–3631.
7 Z. Yang and B. Xu, *J. Mater. Chem.*, 2007, **17**, 2385–2393.
8 S. Kiyonaka, K. Sugiyasu, S. Shinkai and I. Hamachi, *J. Am. Chem. Soc.*, 2002, **124**, 10954–10955.
9 S. Matsumoto, S. Yamaguchi, S. Ueno, H. Komatsu, M. Ikeda, K. Ishizuka, Y. Iko, K. V. Tabata, H. Aoki, S. Ito, H. Noji and I. Hamachi, *Chem.–Eur. J.*, 2008, **14**, 3977–3986.
10 S. Matsumoto, S. Yamaguchi, A. Wada, T. Matsui, M. Ikeda and I. Hamachi, *Chem. Commun.*, 2008, 1545–1547.
11 S. Kiyonaka, S. Shinkai and I. Hamachi, *Chem.–Eur. J.*, 2003, **9**, 976–983.
12 G. Macbeath and S. L. Schreiber, *Science*, 2000, **289**, 1760–1763.
13 D. A. Hall, J. Ptacek and M. Snyder, *Mech. Ageing Dev.*, 2007, **128**, 161–167.
14 D. A. Hall, H. Zhu, X. Zhu, T. Royce, M. Gerstein and M. Snyder, *Science*, 2004, **306**, 482–484.
15 D. N. Gosalia and S. L. Diamond, *Proc. Natl. Acad. Sci. U. S. A.*, 2003, **100**, 8721–8726.
16 S.-i. Tamaru, S. Kiyonaka and I. Hamachi, *Chem.–Eur. J.*, 2005, **11**, 7294–7304.
17 S. Kiyonaka, K. Sada, I. Yoshimura, S. Shinkai, N. Kato and I. Hamachi, *Nat. Mater.*, 2004, **3**, 58–64.
18 Y. Koshi, E. Nakata, H. Yamane and I. Hamachi, *J. Am. Chem. Soc.*, 2006, **128**, 10413–10422.
19 C. R. Bertozzi and L. L. Kiessling, *Science*, 2001, **291**, 2357–2364.
20 R. A. Dwek, *Chem. Rev.*, 1996, **96**, 683–720.
21 I. L. Medintz, A. R. Clapp, H. Mattoussi, R. R. Goldman, B. Fisher and J. M. Mauro, *Nat. Mater.*, 2003, **2**, 630–638.
22 A. Ojida, Y. Mito-oka, M. Inoue and I. Hamachi, *J. Am. Chem. Soc.*, 2002, **124**, 6256–6258.
23 A. Ojida, Y. Mito-oka, K. Sada and I. Hamachi, *J. Am. Chem. Soc.*, 2004, **126**, 2454–2463.
24 I. Yoshimura, Y. Miyahara, N. Kasagi, H. Yamane, A. Ojida and I. Hamachi, *J. Am. Chem. Soc.*, 2004, **126**, 12204–12205.
25 A. Ojida, Y. Miyahara, J. Wongkongkatep, S.-i. Tamaru, K. Sada and I. Hamachi, *Chem.–Asian J.*, 2006, **1**, 555–563.
26 M. Eberhard and P. Erne, *Biochem. Biophys. Res. Commun.*, 1991, **180**, 209–215.
27 J. E. Whitaker, R. P. Haugland and F. G. Prendergast, *Anal. Biochem.*, 1991, **194**, 330–344.
28 G. Cooke and V. M. Rotello, *Chem. Soc. Rev.*, 2002, **31**, 275–286.
29 J. Lavigne and E. V. Anslyn, *Angew. Chem., Int. Ed.*, 2001, **40**, 3118–3130.
30 M. A. Palacios, R. Nishiyabu, M. Marquez and P. Anzenbacher Jr., *J. Am. Chem. Soc.*, 2007, **129**, 7538–7544.
31 N. A. Rakow and K. S. Suslick, *Nature*, 2000, **406**, 710–713.
32 S. Arimori, M. L. Bell, C. S. Oh, K. A. Frimat and T. D. James, *Chem. Commun.*, 2001, 1836–1837.
33 F. M. Raymo and M. A. Cejas, *Org. Lett.*, 2002, **4**, 3183–3185.
34 S. Yamaguchi, T. Yoshimura, T. Kohira, S.-i. Tamaru and I. Hamachi, *J. Am. Chem. Soc.*, 2005, **127**, 11835–11841.
35 M. Cohen, C. Demers, E. P. Gurfinkel, A. G. G. Turpie, G. J. Fromell, S. Goodman, A. Langer, R. M. Califf, K. A. A. Fox, J. Premmereur and F. Bigonzi, *N. Engl. J. Med.*, 1997, **337**, 447–452.
36 D. O. Clegg, D. J. Reda, C. L. Harris, M. A. Klein, J. R. O'Dell, M. M. Hooper, J. D. Bradley, C. O. Bingham, M. H. Weisman, C. G. Jackson, N. E. Lane, J. J. Cush, L. W. Moreland, H. R. Schumacher, C. V. Oddis, F. Wolfe, J. A. Molitor, D. E. Yocum, T. J. Schnitzer, D. E. Furst, A. D. Sawitzke, H. Shi, K. D. Brandt, R. W. Moskowitz and H. J. Williams, *N. Engl. J. Med.*, 2006, **354**, 795–808.
37 A. Wada, S.-i. Tamaru, M. Ikeda and I. Hamachi, *J. Am. Chem. Soc.*, 2009, **131**, 5321–5330.
38 M. Comes, M. D. Marcos, R. Martínez-Mánez, F. Sancenón, J. Soto, L. A. Villaescusa and P. Amorós, *Chem. Commun.*, 2008, 3639–3641.
39 C. Park, K. Oh, S. C. Lee and C. Kim, *Angew. Chem., Int. Ed.*, 2007, **46**, 1445–1457.